# Synergistic retrieval and Complete Data Fusion methods applied to FORUM and IASI-NG simulated measurements

Marco Ridolfi[1,*], Cecilia Tirelli[2,*], Simone Ceccherini[2], Claudio Belotti[1], Ugo Cortesi[2], and Luca Palchetti[1]

[1]Istituto Nazionale di Ottica del Consiglio Nazionale delle Ricerche, Via Madonna del Piano 10, 50019 Sesto Fiorentino, Italy
[2]Istituto di Fisica Applicata "Nello Carrara" del Consiglio Nazionale delle Ricerche, Via Madonna del Piano 10, 50019 Sesto Fiorentino, Italy
[*]These authors contributed equally to this work.

**Correspondence:** Marco Ridolfi (marco.ridolfi@cnr.it) and Simone Ceccherini (s.ceccherini@ifac.cnr.it)

**Abstract.** In the frame of Earth observation remote sensing data analysis, Synergistic Retrieval (SR) and Complete Data Fusion (CDF) are techniques used to exploit the complementarity of the information carried by different measurements sounding the same air mass and / or ground pixel. While more difficult to implement due to the required simultaneous access to measurements originating from different instruments / missions, the SR method is sometimes preferred over the CDF method as the latter relies on a linear approximation of the retrieved states as functions of the true atmospheric and / or surface state.

In this work, we study the performance of the SR and CDF techniques when applied to simulated measurements of the FORUM (Far-infrared Outgoing Radiation Understanding and Monitoring) and the IASI-NG (Infrared Atmospheric Sounding Interferometer - New Generation) missions that will be operational in a few years, from two polar orbiting satellites. The study is based on synthetic measurements generated for the two missions, in clear-sky ~~Antarctic~~ atmospheres. The target parameters of the inversion are the vertical profiles of temperature, water vapour and ozone mixing ratios, surface temperature and spectral emissivity.

We find that for exact matching of the measurements, the results of the SR and CDF techniques differ by less than 1/10 of their errors estimated trough the propagation of measurement noise. For measurements with a realistic mismatch in space and time, the two methods provide more different results. Still in this case, however, the differences between the results are within the error bars due to measurement noise. We conclude that, when applied to FORUM and IASI-NG missions, the two methods are equivalent from the accuracy point of view.

## 1 Introduction

Synergistic Retrieval (SR) and Complete Data Fusion (CDF) are two methods used to combine remote sensing measurements acquired by independent instruments, simultaneously probing the same airmass and / or surface area. Measurements in different parts of the electromagnetic spectrum (e.g ultraviolet, visible, infrared), adopting different acquisition geometries (e.g nadir and limb sounding) have different sensitivities to the vertical distribution of atmospheric and surface variables. For this reason, combining complementary information from different spectral regions and different sensors can significantly improve the

performance of the determined vertical profiles and surface parameters, in terms of both enhanced spatial resolution and ~~errors~~ error reduction.

In the last few decades, the need to advance the knowledge of tropospheric and stratospheric chemical / physical processes stimulated the development of new techniques to fully exploit the synergy of the great number of existing satellite measurements. Recent studies demonstrated the benefits of combining measurements from different sensors operating in different spectral ranges and/or with different observation geometries, by using simulated (Landgraf and Hasekamp, 2007; Worden et al., 2007; Natraj et al., 2011; Costantino et al., 2017; Tirelli et al., 2020; Zoppetti et al., 2021) and real data (Ceccherini et al., 2010b; Cortesi et al., 2016; Kuai et al., 2013; Fu et al., 2013, 2016; Cuesta et al., 2013, 2018; Worden et al., 2015).

The approaches for the combined use of two or more observations of the same portion of atmosphere and / or surface to determine the atmospheric and / or surface state could be divided in two main classes (Aires et al., 2012): the SR and the a posteriori combination of the parameters derived from the inversion of the individual measurements.

The SR is commonly used, as it rigorously combines complementary information of the measurements, see e.g. Landgraf and Hasekamp 2 . The SR, however, requires to integrate into a single inversion system the radiative transfer models capable to simulate the measurements of all the sensors involved in the synergistic inversion. Furthermore, the SR requires the simultaneous access to all the (Level 1) measurements used in the inversion, thus implying the need to handle relevant data volumes. These characteristics complicate the SR implementation and increase the computational resources needed.

The a posteriori techniques, such as data fusion (Ceccherini et al., 2010a) or the Kalman filter (Warner et al., 2014), overcome the main complications implied by the SR method by combining the Level 2 products supplied by the individual retrieval processors of the independent measurements. The CDF method (Ceccherini et al., 2015) can be considered a weighted average of parameters, generalized to the case of averaging kernel matrices (AKMs) different from the identity matrix. The CDF takes advantage of its simple implementation and of its capability to reduce the amount of data involved in the synergistic analysis, and it is able to improve the quality of the operational products of individual instruments in terms of both a reduced total error and an increased number of degrees of freedom (DOFs). Ceccherini et al. (2015) show that CDF and SR provide the same solution, with the same error and number of DOFs, under a) linear approximation of the forward model of each measurement in the range of variability between the solutions of the single retrievals and of the synergistic retrieval and b) assumption of perfectly matching measurements. In this paper, we characterize the differences between SR and CDF results, for realistic conditions that may be encountered in the attempt to combine the complementary measurements of two forthcoming satellite missions: FORUM (Far ~~Infrared~~ infrared Outgoing Radiation Understanding and Monitoring) and IASI-NG (Infrared Atmospheric Sounding Interferometer-New Generation).

FORUM will be the ninth Earth Explorer mission of the European Space Agency ~~(Palchetti et al., 2020)~~(Oetjen, 2019; Palchetti et al., 20 , its launch is scheduled in 2027 on a polar orbiting satellite. FORUM will fly in loose formation with the MetOp-SG-1A satellite, that will host IASI-NG ~~(Crevoisier et al., 2014)~~(Clerbaux and Crevoisier, 2013; Bermudo et al., 2014; Crevoisier et al., 2014; Andrey- . The key instrument of the FORUM mission is a FT (Fourier Transform) spectrometer. It will measure both the Far-Infrared (FIR), and a Mid-Infrared (MIR) portion of the Earth's upwelling spectral radiance (from 100 to 1600 $cm^{-1}$). Conversely, IASI-NG will measure only the MIR spectral range, from 645 to 2760 $cm^{-1}$. The simultaneous exploitation of matching FORUM

and IASI-NG spectra will generate products (namely temperature and $H_2O$ profiles, cloud parameters, surface temperature and spectral emissivity) that will benefit of the information contained in the whole thermal spectrum (from 100 to 2760 $cm^{-1}$, see Ridolfi et al. (2020); Tirelli et al. (2021)).

When FORUM and IASI-NG simulated measurements are combined, usually, the differences between the SR and the CDF solutions are not larger than the retrieval error due to measurement noise. For this reason, to accurately characterize these differences, we base the results of our study on statistically significant sets of test retrievals from simulated observations. A first set of test retrievals uses perfectly matching FORUM and IASI-NG measurements, while a second set uses realistically mismatching measurements. All the synthetic measurements ~~considered~~ used in this paper refer to a clear sky Antarctic winter scenario, with the Earth's surface covered by snow. A dry atmosphere is in fact a pre-requisite to retrieve surface spectral emissivity in the FIR region, a key target for the FORUM mission (Ridolfi et al., 2020). Although less interesting due to the large retrieval errors in FIR surface emissivity, to strengthen the conclusions of the present work, the results of two analogous test experiments carried out at mid- and tropical- latitudes are attached to this paper as supplemental material.

The statistics of the differences between the SR / CDF products and the true state parameters allow to quantify the possible biases and the random errors of the two solutions. For verification purposes, these *ex-post* statistical error estimates can also be compared to the related *ex-ante* predictions provided by the error Covariance Matrices (CMs) of the two solutions. Finally, the statistics of the differences between the SR and CDF solutions quantify the discrepancies between the two methods for realistic forward model linearity, and mismatch between the measurements.

The structure of the paper is as follows. In Section 2, we recall the mathematical background of the SR and the CDF approaches. In Section 3, we describe the characteristics of the FORUM and IASI-NG simulated measurements. In Section 4, we introduce the test scenarios and the retrieval set-up. In Section 5, we discuss the results of the simulated experiments and, finally, in Section 6, we draw the conclusions.

## 2 Methods

We first recall the equations of the SR and CDF approaches. The formalism adopted is based on that of Rodgers (2000).

We indicate with $\mathbf{y}_i$ the vectors including the spectral radiances acquired by FORUM for $i = 1$ and by IASI-NG for $i = 2$, respectively, and with $\mathbf{x}_i$ the state vectors identifying the atmospheres probed by the two measurements. Initially, we assume identical atmospheric states, that is $\mathbf{x}_1 = \mathbf{x}_2$, later we allow for a mismatch between the measurements, both in space and in time, leading to $\mathbf{x}_1 \neq \mathbf{x}_2$. The vectors $\mathbf{x}_i$ and $\mathbf{y}_i$ are linked by:

$$\mathbf{y}_i = \mathbf{F}_i(\mathbf{x}_i) + \epsilon_i \qquad i = 1, 2\,, \tag{1}$$

where $\mathbf{F}_i(\mathbf{x}_i)$ are the forward models and $\epsilon_i$ are the measurement noise errors characterized by the CMs $\mathbf{S}_{yi}$. For the inversion of the two measurements, we use the optimal estimation method (Rodgers, 2000), which obtains the solutions as the ~~minimizer~~ minimizers of the following cost functions:

$$\xi_i^2(\mathbf{x}) = (\mathbf{y}_i - \mathbf{F}_i(\mathbf{x}))^t\, \mathbf{S}_{yi}^{-1}\, (\mathbf{y}_i - \mathbf{F}_i(\mathbf{x})) + (\mathbf{x}_{ai} - \mathbf{x})^t\, \mathbf{S}_{ai}^{-1}\, (\mathbf{x}_{ai} - \mathbf{x}) \qquad i = 1, 2\,, \tag{2}$$

where $\mathbf{S}_{ai}$ are the CMs of the a priori state vectors $\mathbf{x}_{ai}$ used to constrain the retrievals.

The minima of these cost functions are found using the Gauss-Newton iterative formula:

$$\mathbf{x}_{i,k} = \mathbf{x}_{i,k-1} + \left[\mathbf{K}_{i,k-1}^t \mathbf{S}_{yi}^{-1} \mathbf{K}_{i,k-1} + \mathbf{S}_{ai}^{-1}\right]^{-1} \left[\mathbf{K}_{i,k-1}^t \mathbf{S}_{yi}^{-1} \left(\mathbf{y}_i - \mathbf{F}_i(\mathbf{x}_{i,k-1})\right) + \mathbf{S}_{ai}^{-1} \left(\mathbf{x}_{ai} - \mathbf{x}_{i,k-1}\right)\right] \qquad i = 1,2\,, \tag{3}$$

where $k$ indicates the iteration index and $\mathbf{K}_{i,k-1}$ are the Jacobians of the forward models calculated in $\mathbf{x}_{i,k-1}$. Iterations are stopped when the following convergence criterion is fulfilled:

$$\frac{\xi^2(\mathbf{x}_{i,k}) - \xi^2(\mathbf{x}_{i,k-1})}{\xi^2(\mathbf{x}_{i,k-1})} < \zeta\,, \tag{4}$$

where $\zeta$ is a threshold value that in this work is taken equal to ~~$10^{-4}$~~ $3 \times 10^{-4}$. In order to cope with forward model non-linearities, the iterative formula of Eq. (3) is modified with the Levenberg-Marquardt (LM) method (Levenberg, 1944; Marquardt, 1963). Specifically, the diagonal elements of the matrix in the leftmost square brackets of Eq. (3) are multiplied by $(1+\lambda_k)$, where $\lambda_k$ is a positive coefficient, damping the correction applied to the state $\mathbf{x}_{i,k-1}$. At each iteration $k$, $\lambda_k$ is increased or decreased depending on whether the cost function (2) is, respectively, larger or smaller as compared to its value at the previous iteration. To make sure that the LM method does not influence the final solution of the retrieval, we actually check the ~~above mentioned~~ convergence condition only if ~~the LM damping factor is smaller than $10^{-3}$~~ $\lambda_k \leq 10^{-3}$.

We indicate with $\hat{\mathbf{x}}_i$ the solutions of the two retrievals. They are characterized by error CMs ~~and AKMs~~ $\mathbf{S}_i$ and AKMs $\mathbf{A}_i$ given by:

$$\mathbf{S}_i = \left[\mathbf{K}_i^t \mathbf{S}_{yi}^{-1} \mathbf{K}_i + \mathbf{S}_{ai}^{-1}\right]^{-1} \qquad i = 1,2\,, \tag{5}$$

$$\mathbf{A}_i = \left[\mathbf{K}_i^t \mathbf{S}_{yi}^{-1} \mathbf{K}_i + \mathbf{S}_{ai}^{-1}\right]^{-1} \mathbf{K}_i^t \mathbf{S}_{yi}^{-1} \mathbf{K}_i \qquad i = 1,2\,, \tag{6}$$

where $\mathbf{K}_i$ are the Jacobians of the forward models calculated at ~~convergence.~~ the convergence state $\hat{\mathbf{x}}_i$. The noise contributions $\mathbf{S}_{n,i}$ to the CMs of Eq. (5) are given by:

$$\mathbf{S}_{n,i} = \left[\mathbf{K}_i^t \mathbf{S}_{yi}^{-1} \mathbf{K}_i + \mathbf{S}_{ai}^{-1}\right]^{-1} \mathbf{K}_i^t \mathbf{S}_{yi}^{-1} \mathbf{K}_i \left[\mathbf{K}_i^t \mathbf{S}_{yi}^{-1} \mathbf{K}_i + \mathbf{S}_{ai}^{-1}\right]^{-1} \qquad i = 1,2\,, \tag{7}$$

which are obtained by propagating the measurement noise errors $\epsilon_i$ onto the solutions $\hat{\mathbf{x}}_i$.

### 2.1 Synergistic retrieval

The SR is obtained fitting simultaneously the radiances acquired by the two instruments with the forward model simulations, i.e. by minimizing the cost function:

$$\xi^2(\mathbf{x}) = \sum_{i=1}^{2} \left(\mathbf{y}_i - \mathbf{F}_i(\mathbf{x})\right)^t \mathbf{S}_{yi}^{-1} \left(\mathbf{y}_i - \mathbf{F}_i(\mathbf{x})\right) + \left(\mathbf{x}_a - \mathbf{x}\right)^t \mathbf{S}_a^{-1} \left(\mathbf{x}_a - \mathbf{x}\right)\,, \tag{8}$$

where $\mathbf{S}_a$ is the error CM of the a priori state $\mathbf{x}_a$ assumed for the SR.

As in the case of the inversion of a single measurement, the minimum of this cost function is found using the Gauss-Newton iterative formula that, in the case of the SR, takes the form:

$$\mathbf{x}_k = \mathbf{x}_{k-1} + \left[\sum_{i=1}^{2} \mathbf{K}_{i,k-1}^t \mathbf{S}_{\mathrm{y}i}^{-1} \mathbf{K}_{i,k-1} + \mathbf{S}_{\mathrm{a}}^{-1}\right]^{-1} \left[\sum_{i=1}^{2} \mathbf{K}_{i,k-1}^t \mathbf{S}_{\mathrm{y}i}^{-1} \left(\mathbf{y}_i - \mathbf{F}_i(\mathbf{x}_{k-1})\right) + \mathbf{S}_{\mathrm{a}}^{-1} \left(\mathbf{x}_{\mathrm{a}} - \mathbf{x}_{k-1}\right)\right] . \tag{9}$$

Also in this case, the used formula is modified with the LM method and we take care of ending the iterations with a sufficiently small LM damping parameter.

We indicate with $\hat{\mathbf{x}}$ the SR solution. It is characterized by error CM ~~and AKM~~ $\mathbf{S}$ and AKM $\mathbf{A}$ given by:

$$\mathbf{S} = \left[\sum_{i=1}^{2} \mathbf{K}_i^t \mathbf{S}_{\mathrm{y}i}^{-1} \mathbf{K}_i + \mathbf{S}_{\mathrm{a}}^{-1}\right]^{-1} \tag{10}$$

$$\mathbf{A} = \left[\sum_{i=1}^{2} \mathbf{K}_i^t \mathbf{S}_{\mathrm{y}i}^{-1} \mathbf{K}_i + \mathbf{S}_{\mathrm{a}}^{-1}\right]^{-1} \sum_{i=1}^{2} \mathbf{K}_i^t \mathbf{S}_{\mathrm{y}i}^{-1} \mathbf{K}_i \, . \tag{11}$$

If the two measurements do not refer to the same atmosphere because of temporal and / or spatial mismatches, then the two state vectors $\mathbf{x}_1$ and $\mathbf{x}_2$ are different. In this case we can write:

$$\mathbf{y_2} = \mathbf{F}_2(\mathbf{x}_2 - \mathbf{x}_1 + \mathbf{x}_1) + \epsilon_2 \approx \mathbf{F}_2(\mathbf{x}_1) + \mathbf{K}_2(\mathbf{x}_2 - \mathbf{x}_1) + \epsilon_2 = \mathbf{F}_2(\mathbf{x}_1) + \epsilon_2{}' \, , \tag{12}$$

where we have assumed the difference $\mathbf{x}_2 - \mathbf{x}_1$ to be sufficiently small so that an expansion to the first order is sufficiently accurate, and have introduced the quantity $\epsilon_2{}'$, given by:

$$\epsilon_2{}' = \mathbf{K}_2(\mathbf{x}_2 - \mathbf{x}_1) + \epsilon_2 \, . \tag{13}$$

From Eq. (12), we see that $\mathbf{y}_2$ (the radiances acquired by IASI-NG) can be seen as a measurement of $\mathbf{x}_1$ (the atmospheric state sounded by FORUM) with an error $\epsilon_2{}'$ greater than $\epsilon_2$. If we introduce the mismatch CM $\mathbf{S}_{\mathrm{M}}$ of $\mathbf{x}_2 - \mathbf{x}_1$, characterizing the statistical distribution of the differences between the atmospheric states sounded by the two instruments, then the CM $\mathbf{S}'_{\mathrm{y}2}$ of $\epsilon_2{}'$ is given by:

$$\mathbf{S}'_{\mathrm{y}2} = \mathbf{S}_{\mathrm{y}2} + \mathbf{K}_2 \mathbf{S}_{\mathrm{M}} \mathbf{K}_2^t \, . \tag{14}$$

Therefore, in the presence of a mismatch between the two measurements, we still assume that both instruments are sounding the same atmospheric state $\mathbf{x}_1$, however, in the SR we assign to $\mathbf{y}_2$ the error CM $\mathbf{S}'_{\mathrm{y}2}$, i.e. a larger error as compared to the original one described by $\mathbf{S}_{\mathrm{y}2}$.

### 2.2 Complete Data Fusion ~~(CDF)~~

The CDF uses the results of the individual retrievals and its solution is obtained by minimizing the following cost function (Ceccherini et al., 2015):

$$\xi^2_{\mathrm{CDF}}(\mathbf{x}) = \sum_{i=1}^{2} \left(\boldsymbol{\alpha}_i - \mathbf{A}_i \mathbf{x}\right)^t \mathbf{S}_{\mathrm{n},i}^{-1} \left(\boldsymbol{\alpha}_i - \mathbf{A}_i \mathbf{x}\right) + \left(\mathbf{x}_{\mathrm{a}} - \mathbf{x}\right)^t \mathbf{S}_{\mathrm{a}}^{-1} \left(\mathbf{x}_{\mathrm{a}} - \mathbf{x}\right) \, , \tag{15}$$

where

$$\boldsymbol{\alpha}_i = \hat{\mathbf{x}}_i - (\mathbf{I} - \mathbf{A}_i)\mathbf{x}_{ai} \,, \tag{16}$$

$\mathbf{I}$ is the identity matrix and $\mathbf{S}_\mathrm{a}$ is the error CM of the a priori state $\mathbf{x}_\mathrm{a}$ that constrains the CDF solution.

From Eq. (15) we see that, differently from the SR cost function of Eq. (8), the cost function of the CDF is a quadratic form of $\mathbf{x}$, therefore, its minimum can be found analytically without the need of an iterative procedure. Imposing the gradient of the cost function $\xi^2_\mathrm{CDF}(\mathbf{x})$ to be zero, we obtain the CDF solution $\mathbf{x}_\mathrm{f}$ as:

$$\mathbf{x}_\mathrm{f} = \left( \sum_{i=1}^{2} \mathbf{A}_i^t \mathbf{S}_{\mathrm{n},i}^{-1} \mathbf{A}_i + \mathbf{S}_\mathrm{a}^{-1} \right)^{-1} \left( \sum_{i=1}^{2} \mathbf{A}_i^t \mathbf{S}_{\mathrm{n},i}^{-1} \boldsymbol{\alpha}_i + \mathbf{S}_\mathrm{a}^{-1} \mathbf{x}_\mathrm{a} \right) \,, \tag{17}$$

that is characterized by error CM ~~and AKM~~ $\mathbf{S}_\mathrm{f}$ and AKM $\mathbf{A}_\mathrm{f}$ given by:

$$\mathbf{S}_\mathrm{f} = \left( \sum_{i=1}^{2} \mathbf{A}_i^t \mathbf{S}_{\mathrm{n},i}^{-1} \mathbf{A}_i + \mathbf{S}_\mathrm{a}^{-1} \right)^{-1} \tag{18}$$

$$\mathbf{A}_\mathrm{f} = \left( \sum_{i=1}^{2} \mathbf{A}_i^t \mathbf{S}_{\mathrm{n},i}^{-1} \mathbf{A}_i + \mathbf{S}_\mathrm{a}^{-1} \right)^{-1} \sum_{i=1}^{2} \mathbf{A}_i^t \mathbf{S}_{\mathrm{n},i}^{-1} \mathbf{A}_i \,. \tag{19}$$

If the two measurements do not exactly coincide both in space and time, we allow for this mismatch by introducing a coincidence error according to the approach described in Ceccherini et al. (2018). Coherently with what is done in the SR, we consider the measurement of IASI-NG as a measurement of the atmospheric state $\mathbf{x}_1$ sounded by FORUM, and add the coincidence error to the IASI-NG measurement error. Specifically, in the presence of a mismatch between the measurements, we still use the above mentioned equations for the CDF, with $\mathbf{S}_{\mathrm{n},2}$ replaced by $\mathbf{S}'_{\mathrm{n},2}$, given by:

$$\mathbf{S}'_{\mathrm{n},2} = \mathbf{S}_{\mathrm{n},2} + \mathbf{A}_2 \mathbf{S}_\mathrm{M} \mathbf{A}_2^t \,. \tag{20}$$

### 2.3 Differences between SR and CDF approaches

First, let us consider the case of perfectly matching measurements. If in the range of variability of the solutions of the individual retrievals and of the SR, the linear approximation can be applied to the forward model of both measurements, then the two methods are equivalent, as demonstrated in the appendix of Ceccherini et al. (2015). On the other hand, when the forward models of the measurements exhibit significant non-linearities in the range of variability of the solutions of the individual retrievals and of the SR, a difference is expected between SR and CDF results. In this case, the SR should provide a more accurate result as the iterative procedure of Eq. (9) takes correctly into account the non-linearities and models the interactions between the information flows arising from the two contributing measurements (Aires et al., 2012).

Now, let us consider the case of measurements not perfectly matching. In the SR, the CM $\mathbf{S}_{\mathrm{y}2}$ of the radiances of IASI-NG is increased as described by Eq. (14). Then, neglecting the non-linearities, the SR should be equivalent to the CDF of the result

of the FORUM retrieval and the result of the retrieval of IASI-NG with CM $\mathbf{S}'_{y2}$. The IASI-NG retrieval obtained with $\mathbf{S}'_{y2}$ produces different state vector, CM and AKM with respect to those obtained with $\mathbf{S}_{y2}$. To deal with the mismatch, in the CDF approach only the CM of the IASI-NG retrieval is changed according to Eq. (20), leaving the state vector and the AKM equal to those obtained in the absence of a mismatch. The two approaches, therefore, are slightly different and we expect a difference in the results.

## 3 Simulated measurements

As mentioned in Sect. 1, our tests are based on simulated measurements from two forthcoming satellite missions: FORUM and IASI-NG. The two experiments will be installed on two different satellite platforms operating in *loose formation*. FORUM will fly on a Sun-Synchronous Polar orbiting satellite. The orbit inclination is planned to be of 98.7°, with a mean local solar time of 09:30 hours at descending node, and satellite altitude of about 830 km. The orbit repeat cycle will be of 29 days. These orbit features coincide with those of the MetOp-SG-1A that will host IASI-NG.

The key instrument of the FORUM mission will be a FT spectrometer measuring the spectrum of the upwelling Earth's Outgoing Longwave Radiation (OLR) by looking at nadir (Oetjen, 2019; Palchetti et al., 2020). The ground pixel will be a circle, with a diameter of approximately 15 km. During the acquisition time (≈8 s), the ground pixel will be kept fixed with a continuous adjustment of the pointing angle to compensate for the satellite motion (the so called *step and stare* technique). No across-track scanning is foreseen. The resulting distance between neighbouring ground pixels will be approximately of 100 km. FORUM measured interferograms will be processed to get geolocated and calibrated spectral radiances in the interval from 100 to 1600 $\mathrm{cm}^{-1}$, with (unapodized) spectral resolution of 0.5 $\mathrm{cm}^{-1}$ (Full Width at Half Maximum, FWHM of the response function). The sampling step of the spectrum will be $\approx 0.36$ $\mathrm{cm}^{-1}$. As for NESR (Noise Equivalent Spectral Radiance) of the unapodized spectrum, we assume the *goal* instrument requirement of 40 nW/($\mathrm{cm}^2$ sr $\mathrm{cm}^{-1}$) in the range between 200 and 800 $\mathrm{cm}^{-1}$ and 100 nW/($\mathrm{cm}^2$ sr $\mathrm{cm}^{-1}$) elsewhere. The ARA (Absolute Radiometric Accuracy) of the measured spectral radiance is required to be much smaller than the NESR (see Oetjen (2019); Ridolfi et al. (2020) and Fig. 1 introduced later).

Like FORUM, IASI-NG will also measure the upwelling spectral radiance, however, its focus will be on the MIR region, with a coverage from 645 to 2760 $\mathrm{cm}^{-1}$. IASI-NG will exploit a detector array to measure, simultaneously, the spectra upwelling from sets of 4×4 ground pixels with a diameter of 12 km. Each set of 16 pixels constitutes the FOR (Field Of Regard) of IASI-NG. The instrument pointing will be scanned across track, to get a global coverage of the measurements by acquiring up to 7 FORs on both sides of the orbit track. According to Crevoisier et al. (2014), IASI-NG will provide an apodized spectrum with response given by a Gaussian function with FWHM equal to 0.25 $\mathrm{cm}^{-1}$ (the spectral resolution). The sampling step of the spectrum will be of 0.125 $\mathrm{cm}^{-1}$ and its NESR will be half of the NESR typical of the current IASI instrument onboard of MetOp (Crevoisier et al., 2014). The ARA of IASI-NG is specified to be less than 0.25 K ($2\sigma$) at blackbody temperature of 280 K.

Figure 1 is a summary of the NESR and ARA errors expected for FORUM and IASI-NG measurements as a function of wavenumber. As we can see, while not extended to the FIR region, and affected by a non-negligible systematic error (ARA),

IASI-NG is far less noisy than FORUM in the atmospheric window region (780 – 980 $cm^{-1}$). Since this is the spectral interval that carries most of the information on surface temperature, this feature of IASI-NG is of utmost importance to disentangle the retrieved surface emissivity and temperature.

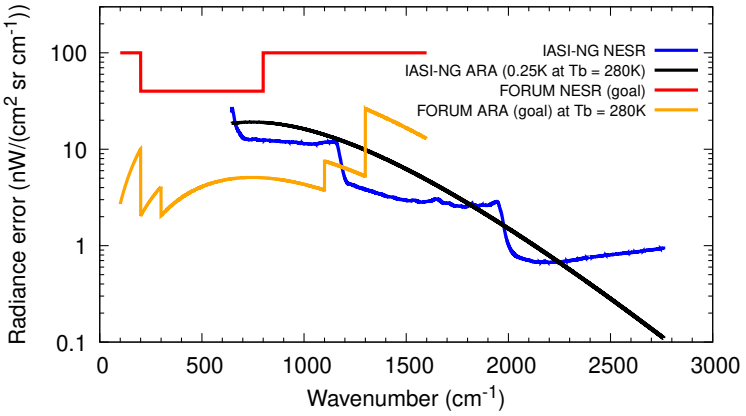


**Figure 1.** FORUM and IASI-NG NESR and ARA requirements. The ARA errors, originally given in brightness temperature, are converted to radiance units assuming a scene temperature of 280 K. The plotted curves refer to $1\sigma$ error bounds.

To generate a synthetic measurement we proceed as follows. The atmospheric state is first defined by setting the vertical profiles of temperature and constituent's Volume Mixing Ratio (VMR) at a set of fixed pressure levels. The surface is then defined by setting the values of surface pressure, temperature, height above sea level, and spectral emissivity (on a 5 $cm^{-1}$ grid). These inputs are then passed to $\sigma-$~~RTM~~IASI, a fast monochromatic, parametrized forward model developed at University of Basilicata, Italy ~~(Amato et al., 2002; Liuzzi et al., 2017)~~(Amato et al., 2002; Liuzzi et al., 2017; Masiello et al., 2022). From these inputs, $\sigma-$~~RTM~~ IASI computes the outgoing spectral radiance in the interval from 80 to 2780 $cm^{-1}$, with a wavenumber step as fine as 0.01 $cm^{-1}$. The instrumental effects are then simulated by convolving this radiance with the Apodized Instrument Spectral Response Function (AISRF) and adding apodized measurement noise. For FORUM, we assume an AISRF given by a Norton-Beer strong apodizing function (Norton and Beer, 1976, 1977; Naylor and Tahic, 2007) with a Maximum Optical Path Difference (MOPD) such that 1/(2 MOPD) = 0.413 $cm^{-1}$, as expected for an unapodized spectral response given by a *sinc* function with FWHM = 0.5 $cm^{-1}$ = 1.21/(2 MOPD). For IASI-NG, we assume a Gaussian AISRF with a FWHM of 0.25 $cm^{-1}$.

The measurement error covariance matrices $\mathbf{S}_{y1}$ and $\mathbf{S}_{y2}$ of FORUM and IASI-NG measurements are then built considering the NESR figures specified above and the correlations implied by the apodization process. The ARA systematic errors are not considered in the test cases presented in this work. On one hand, being smaller or of the same order of the NESR, the ARA error has negligible impact on the convergence of the individual retrievals and on their eventual ill-conditioning, thus, discarding this error component does not change the performance of the individual inversions. On the other hand, the ARA error may introduce biases on the retrieved parameters that may show up in the averages. These biases would sum up to the

other possible retrieval systematic effects (like convergence error) that we want to keep negligibly small when focusing on the study of the differences between SR and CDF approaches.

Pseudo-random noise extracted from a multi-variate Gaussian distribution consistent with the measurement error CM is finally added to the simulated apodized spectral radiances.

### 3.1 Mismatches between FORUM and IASI-NG measurements

FORUM orbit will be adjusted to match the MetOp-SG-1A orbit, however, the matching between the two orbits will not be perfect. Necessarily, there will be a time lag between the two satellites. Currently, this lag is specified to be smaller than 1 min. Secondly, the ground tracks of the two satellites will not coincide exactly. The maximum distance between the FORUM and MetOp-SG-1A ground tracks is however required to be smaller than 300 km. These conditions are usually referred as the requirements for the two satellites to fly in *loose formation*.

Since FORUM will measure only a single ground pixel in the nadir-looking geometry, its measurements will match only the IASI-NG pixels closest to satellite ground track. The distance between the centres of IASI-NG pixels ranges from ≈32 km in the area close to the sub-satellite track, to ≈87 km for the FORs at the ends of the across-track scan. Simulations actually show that, assuming a distance of 300 km between the ground tracks of the two orbits, the maximum distance between two matching FORUM and IASI-NG pixels will be of 26 km, occurring in the unlucky case in which the FORUM pixel falls between two contiguous IASI-NG FORs. On average, the distance between matching pixel centres will be around 10 km, the actual value depending on latitude.

When dealing with mismatching measurements, we always assume the worst case of 1 min time lag and 26 km distance between the closest FORUM and IASI-NG soundings. At these time- and space- scales, the inconsistency between the spectra measured by the two instruments may be assumed to arise mainly from the different temperature and $H_2O$ VMR profiles, and the different surface temperatures and emissivities. The two measurements may also be inconsistent due to a different cloud coverage, however, as shown in Ridolfi et al. (2020), this occurrence degrades quite significantly the advantages of the synergy. Most likely, in operational conditions the occurrence of different cloud coverage in the two measurements will be detected from the analysis of co-located imager measurements (available for both FORUM and IASI-NG) and, in this case, neither the SR nor the CDF will be performed. Having in mind this possible strategy, and considering the additional complications connected with the retrieval of cloud parameters, we decided to limit the present study to clear-sky atmospheres.

The objective of both SR and CDF is to get the best estimate of the atmospheric and surface state corresponding to the air mass and the ground pixel sounded by FORUM, with the help of the IASI-NG measurement. If IASI-NG is not probing the same air mass or ground pixel as FORUM, a *mismatch error* should be attributed both to the IASI-NG spectrum when used in the SR, and to the state vector retrieved from the IASI-NG-only measurement, when this is used in the CDF. The mismatch

error assigned to the IASI-NG state vector is represented by a block-diagonal CM $\mathbf{S}_{\mathrm{M}}$:

$$\mathbf{S}_{\mathrm{M}} = \begin{pmatrix} \mathbf{S}_{\mathrm{T}} & 0 & 0 & 0 & 0 \\ 0 & \mathbf{S}_{\mathrm{Ts}} & 0 & 0 & 0 \\ 0 & 0 & \mathbf{S}_{\mathrm{H}} & 0 & 0 \\ 0 & 0 & 0 & \mathbf{S}_{\mathrm{O_3}} & 0 \\ 0 & 0 & 0 & 0 & \mathbf{S}_{\mathrm{e}} \end{pmatrix}. \tag{21}$$

Each block of this matrix is associated to a specific section of the state-vector, the various sections describe, respectively: the temperature profile ($\mathbf{S}_{\mathrm{T}}$), surface temperature ($\mathbf{S}_{\mathrm{Ts}}$), $H_2O$ profile ($\mathbf{S}_{\mathrm{H}}$), $O_3$ profile ($\mathbf{S}_{\mathrm{O_3}}$) and spectral emissivity ($\mathbf{S}_{\mathrm{e}}$).

We estimate the error covariance matrices $\mathbf{S}_{\mathrm{T}}$, $\mathbf{S}_{\mathrm{Ts}}$ and $\mathbf{S}_{\mathrm{H}}$ on the basis of the atmospheric and surface fields extracted from the ERA5 reanalysis (Hersbach et al., 2020) for the days from 19 to 21 June 2007. The data refer to a circular area with a radius of 140 km, over the Antarctic plateau. The area is centred around the geographical location (82.861°S, 71.667°E) and the time corresponding to the reference scenario used in the test experiments presented later (see Sect. 4). The data are provided hourly, on a regular latitude-longitude grid of $0.25° \times 0.25°$. Profiles are given on 37 pressure levels, in the range from 1000 to 1 hPa. Within the selected 140 km radius area, we consider 25 different circular sub-areas, with a radius of 26 km (the mismatch threshold). For each of these sub-areas, and for each pressure level, we compute the squared deviations of the profile values from the sub-area average. We finally average all the obtained squared deviations to get the space variances used later to build $\mathbf{S}_{\mathrm{M}}$. The time variability is estimated in a similar way. First, we compute the root mean square (rms) of the hourly variations of profiles relating to selected grid points within the 140 km radius area. This hourly rms is then linearly down-scaled to estimate the variability corresponding to 1 min time lag between the FORUM and IASI-NG measurements, and then squared to get the covariance of the time variability. The total mismatch variances are obtained by summing up the variances owing to space- and time- variabilities. Finally, the total error covariance matrices $\mathbf{S}_{\mathrm{T}}$, $\mathbf{S}_{\mathrm{Ts}}$ and $\mathbf{S}_{\mathrm{H}}$ are built assuming these total mismatch variances and correlations between profile levels decreasing exponentially, with a vertical correlation length of 5 km.

In $\mathbf{S}_{\mathrm{M}}$, we set $\mathbf{S}_{\mathrm{O_3}} = 0$ for two reasons: first, as compared to the other parameters, ozone shows only a very limited variability within the mismatch margins considered, second, we retrieve the ozone profile as an auxiliary parameter to limit its interference error on the other target parameters, ozone on its own is not considered a key target parameter for FORUM. Finally, we estimate $\mathbf{S}_{\mathrm{e}}$ by applying the statistical estimator of the covariance to a set of 19 surface emissivity models from Huang et al. (2016), preliminarily interpolated to the actual retrieval grid. In the SR, we use Eq. (14) to map the error $\mathbf{S}_{\mathrm{M}}$ onto the IASI-NG spectrum.

## 4 Test scenario and retrieval setup

We illustrate the results of two main sets of tests. The first set is based on the assumption of perfectly matching FORUM and IASI-NG measurements. In the second set, this assumption is dropped and the matching errors described in Sect. 3.1 are considered. In both cases, the objective is to characterize the differences between the results obtained from the SR and CDF approaches. Since these differences are usually smaller or of the order of the retrieval error due to measurement noise, we

perform a statistical analysis of a relatively large set of trials obtained by changing the seeds used to initialize the pseudo-random numbers generator that produces the measurement noise and the perturbed atmospheres. Some features are common to all the test cases presented. For example, the retrieval state vector:

$$\mathbf{x} = \begin{pmatrix} (\mathbf{x}_{\mathrm{T}}(p_1), \ldots, \mathbf{x}_{\mathrm{T}}(p_{61}))^t \\ \mathbf{x}_{\mathrm{T_s}} \\ (\mathbf{x}_{\mathrm{H2O}}(p_1), \ldots, \mathbf{x}_{\mathrm{H2O}}(p_{61}))^t \\ (\mathbf{x}_{\mathrm{O3}}(p_1), \ldots, \mathbf{x}_{\mathrm{O3}}(p_{61}))^t \\ (\mathbf{x}_{\mathrm{e}}(\nu_1), \ldots, \mathbf{x}_{\mathrm{e}}(\nu_{63}))^t \end{pmatrix} \tag{22}$$

has always the same set of elements, describing the state of the atmosphere and of the surface sounded. It includes the profiles of temperature (~~$T(p_k)$~~ $(\mathbf{x}_{\mathrm{T}}(p_1), \ldots, \mathbf{x}_{\mathrm{T}}(p_{61}))^t$), $H_2O$ and $O_3$ VMRs (~~$\mathbf{x}_{\mathrm{H2O}}(p_k)$ and $\mathbf{x}_{\mathrm{O3}}(p_k)$~~ $(\mathbf{x}_{\mathrm{H2O}}(p_1), \ldots, \mathbf{x}_{\mathrm{H2O}}(p_{61}))^t$ and $(\mathbf{x}_{\mathrm{O3}}(p_1), \ldots, \mathbf{x}_{\mathrm{O3}}(p_{61}))^t$, respectively), which are represented on a fixed pressure grid of 61 levels in the range from 1013 to 0.005 hPa ($p_k$ with $k = 1, \ldots, 61$). Surface temperature ~~$T_s$~~ $\mathbf{x}_{\mathrm{T_s}}$ and spectral emissivity ~~$\epsilon(\nu_h)$~~ $(\mathbf{x}_{\mathrm{e}}(\nu_1), \ldots, \mathbf{x}_{\mathrm{e}}(\nu_{63}))^t$ are also included in the state vector. Surface spectral emissivity modulates the surface emission (black-body at temperature ~~$T_s$~~ $\mathbf{x}_{\mathrm{T_s}}$) and the surface reflectivity (surface is assumed specular in our model), therefore we expect poor sensitivity to this parameter in spectral intervals where the atmosphere is a strong absorber. For this reason~~we retrieved~~, we retrieve emissivity in the range from 100 to 2200 $\mathrm{cm}^{-1}$ on a fixed, irregular, wavenumber grid ~~$\nu_h$~~ $\nu_1, \ldots, \nu_{63}$, tuned on the basis of the sensitivity of the measured spectral radiance to this target parameter. Specifically, the retrieval grid step is 20 $\mathrm{cm}^{-1}$ from 300 to 1200 $\mathrm{cm}^{-1}$ and 50 $\mathrm{cm}^{-1}$ in the intervals from 100 to 300 $\mathrm{cm}^{-1}$ and from 1600 to 2200 $\mathrm{cm}^{-1}$. Moreover, emissivity is not retrieved within the interval from 620 to 720 $\mathrm{cm}^{-1}$, where the strong $CO_2$ absorption band makes the atmosphere fully opaque and, thus, the measured spectral radiance is not sensitive to the surface parameters. In the radiative transfer computations, surface emissivity is assumed to change linearly between the retrieved grid points. It should be noted that, while the $H_2O$ VMR profile and the FIR surface spectral emissivity of Polar regions are key targets for the FORUM mission, the other parameters of the state vector are retrieved only as auxiliary information to preserve the accuracy of the key targets.

Another feature common to all the presented test ~~cases are the errors $\mathbf{S}_a$~~ retrievals is the method used to build the error CMs of the a priori ~~estimate $\mathbf{x}_a$~~ estimates of the state vector. The a priori errors of vertical distribution profiles and of surface temperature coincide with the background errors assumed at the UK MetOffice when the current IASI measurements are assimilated in their Numerical Weather Prediction (NWP) system. The specific values of a priori errors are shown in the figures presented later. Regarding the a priori error of surface emissivity, this is set equal to 0.1 in the spectral range covered by the measurements included in the inversion and equal to an arbitrarily small value ($10^{-4}$) in the range not covered by the measurements (e.g. from 1600 to 2200 $\mathrm{cm}^{-1}$ in FORUM-only inversions). The large a priori error of 0.1 in the spectral region covered by the measurements permits to avoid any significant bias that may be introduced by the OE approach in the regions where the measurements are sensitive to emissivity. Conversely, the small a priori error in the regions not covered by the measurements ties the retrieved emissivity to its a priori value (equal to 0.99 in all the presented cases), thus avoiding retrieval instabilities. This trick of using an a priori emissivity error dependent on the set of measurements included in the inversion, allows to use the same emissivity retrieval grid in FORUM-only, IASI-NG-only and synergistic FORUM + IASI-NG retrievals,

thus making easier the implementation the CDF technique and its comparison to the SR. ~~The a priori $\mathbf{x}_a$ is also always~~ In all the retrievals, the a priori estimate of the state vector is also used as initial guess ~~of the retrieval~~ to start the iterations.

As shown in Ridolfi et al. (2020), due to the presence of strong $H_2O$ absorption bands, the FIR emissivity will be retrievable with sufficiently small error only in the presence of dry atmospheres. For this reason, ~~we base our tests~~ the tests presented in this paper are based on a reference clear-sky atmospheric scenario corresponding to winter conditions over the Antarctic Plateau (82.861°S, 71.667°E, 3600 m a.m.s.l., 20 June 2007) covered by coarse snow (Huang et al., 2016). This scenario (#16) was selected out of a set of 5000 diverse profiles sampled from the outputs of the NWP model of the European Center for Medium-range Weather Forecasts (ECMWF) available from the European Organisation for the Exploitation of Meteorological Satellites (EUMETSAT) NWP Satellite Application Facilities (for data and related documentation, see: `www.nwpsaf.eu/-site/software/atmospheric-profile-data/`). These profiles are considered as representative of the full range of the atmospheric variability, spanning different seasons, latitudes and surface types. The dataset includes vertical distributions of temperature and VMR of $H_2O$, $CO_2$, $O_3$, $N_2O$, CO, and $CH_4$ as a function of pressure. For each profile, the database also includes information on geolocation and time of the year, the surface pressure, temperature and land / sea classification. Profiles of gases not included in the above list, but needed for accurate simulation of atmospheric spectra, were extracted from the *Initial Guess for Level 2* (IG2) climatology developed for MIPAS (Michelson Interferometer for Passive Atmospheric Sounding) retrievals (Remedios et al., 2007). In the following we refer to this reference atmospheric and surface state to as $\mathbf{x}_0$.

To reinforce the conclusions of our analysis, additional test experiments were also carried out at mid- and at tropical-latitudes. Although at these latitudes the retrieval of FIR surface emissivity is more challenging due to the increased opacity of the atmosphere, the behaviour of the SR and CDF methods is actually very similar to that observed with the polar atmospheres considered here. Thus, the results of those experiments are supplied only as supplemental material.

# 5 Results

## 5.1 Results in case of perfectly matching measurements

In the first part of the study, we carried out a set of test retrievals emulating an idealized situation in which both FORUM and IASI-NG measure, with perfect matching, for 900 times, the same area over the Antarctic Plateau, covered by snow with coarse grains. In occasion of each of the measurements, surface temperature and the atmospheric ~~composition~~ state change stochastically with respect to the reference $\mathbf{x}_0$. The stochastic changes comply with the local seasonal variability CM $\mathbf{S}_S$, derived from a 3-months record of ERA5 profiles relating to the grid point closest to the reference location of $\mathbf{x}_0$. The synthetic noise applied to the measurements also changes from measurement to measurement. Since we consider the a priori atmospheric and surface states as extracted from timely updated ECMWF analyses, the a priori estimates for the retrieval also change from measurement to measurement.

More in detail, we repeat ~~900~~ for $j = 1, \ldots, 900$ times the following procedure. We generate FORUM and IASI-NG synthetic observations assuming for both measurements the same ~~set of $\mathbf{T}(p)$, $T_s$, $\mathbf{x}_{H2O}(p)$ and $\mathbf{x}_{O3}(p)$~~ true surface temperature and atmospheric state $\mathbf{x}_{t1,j}$ obtained by applying ~~a random perturbation to the reference values in~~ to $\mathbf{x}_0$ ~~. The applied perturbation~~

~~is consistent with the error CMs that constitute the blocks on the main diagonal of $\mathbf{S}_M/2$ (the reason of why in this application we halve $\mathbf{S}_M$ will be clear from Sect 5.2)~~ a random perturbation ($\delta_{\mathbf{S}_S}(j)$) belonging to a multi-variate distribution with CM $\mathbf{S}_S$. The surface spectral emissivity used to generate ~~the~~ both observations is the reference ~~a~~ coarse snow emissivity spectrum published in Huang et al. (2016). The noise added to FORUM and IASI-NG synthetic observations is consistent with the respective noise error CMs $\mathbf{S}_{y1}$ and $\mathbf{S}_{y2}$. As a priori estimates for surface temperature and for the profiles of temperature, $H_2O$ and $O_3$ VMRs in $\mathbf{x}_{a,j}$, we use values obtained by applying to the true values in $\mathbf{x}_{t1,j}$ a stochastic perturbation ~~with error CM $\mathbf{S}_a$ to the reference value in $\mathbf{x}_0$~~compliant with the a priori error CM. The a priori emissivity estimate is constant versus wavenumber and equal to 0.99. For the generation of each stochastic vector, the routine producing pseudo-random numbers is always re-initialized using the current date / time expressed in nanoseconds. Finally, we carry out the retrievals from FORUM-only, IASI-NG-only and FORUM+IASI-NG (~~synergistic, $\hat{\mathbf{x}}$~~$\hat{\mathbf{x}}_j$, synergistic) measurements and compute the CDF result ~~$\mathbf{x}_f$~~ $\mathbf{x}_{f,j}$ starting from FORUM-only and IASI-NG-only retrieved state vectors.

After these 900 runs, we evaluate both the average and the standard deviation of the differences between the synergistic / fused results and the true values used for the generation of synthetic observations. The average differences quantify the product's bias, while the standard deviation of the differences is an (ex-post) estimate of the product error which, in principle, should equal the product error estimated (ex-ante) with the error CMs (see Eq's 10 and 18). The standard error of the average, i.e. the standard deviation of the differences divided by the square root of the number of trials ($\sqrt{900} = 30$, in this case) is useful to evaluate whether the determined bias is statistically significant.

Figure 2 shows the 900 trials average of a priori (green), true (blue), CDF (black) and SR (magenta) profiles. Error bars represent the average profile errors as evaluated from the error CMs of Eq's (10) and (18). Shadowed areas represent the standard deviation of SR and CDF profiles. Panel (a) refers to the temperature profile and to surface temperature (bottom symbols in the plot). Panels (~~b~~c) and (~~c~~e) refer to the $H_2O$ VMR and surface spectral emissivity profiles, respectively. The *true* profiles used to generate the synthetic observations vary within the local seasonal variability represented by the CM $\mathbf{S}_S$, the resulting standard deviations of temperature and of the $H_2O$ VMR profiles are plotted in panels (b) and (d). This figure is useful for a first visual inspection of the profiles used and of their variability, however, the differences between the various profiles are so small that can not be appreciated~~in these plots~~. With the aim to quantify the agreement of CDF and SR results with the ~~reference or *true* profilesthat were used to generate the synthetic observations~~true profiles, Fig. 3 shows the average differences between CDF and true profiles (black), and between SR and true profiles (magenta). Dashed lines represent the average error of CDF (black) and of SR (magenta) solutions, as evaluated from the error CMs of Eq's (10) and (18). Shadowed areas represent the standard deviations of the profile differences. From this figure we see that the biases of both the CDF and SR solutions (solid black and magenta lines) are much smaller than the average profile errors (dashed lines). In turn, these latter errors, almost identical for the CDF and the SR solutions, generally agree very well with the ex-post error estimation provided by the standard deviation of the differences (shadowed areas). An expected exception occurs for surface emissivity in the spectral regions below 300 $cm^{-1}$ and between 1550 and 1700 $cm^{-1}$, where the sensitivity of the measurements to the surface state is very limited. In these regions, the error evaluated from the standard deviation of the differences is smaller than the error predicted by the CMs because here, both the CDF and the SR solutions are strongly tied to the a priori value that, only

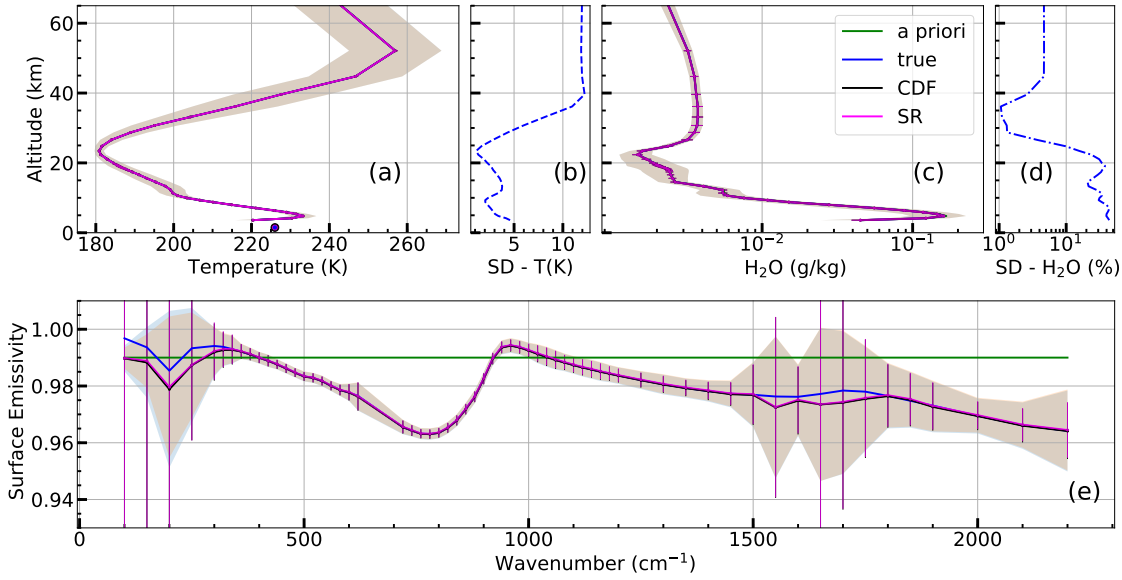


**Figure 2.** Case of perfectly matching measurements. Average on the 900 trials, of a priori (green), true (blue), CDF (black) and SR (magenta) profiles. Panel (a) refers to the temperature profile and to surface temperature (bottom symbol in the plot). Panels (c) and (e) refer to the $H_2O$ VMR and to the surface spectral emissivity profiles, respectively. Error bars represent the average profile errors as evaluated from the error CMs of Eq's (10) and (18). Shadowed areas represent the SR and CDF profiles standard deviation. ~~Panel (a) refers to~~ The standard deviations of the true profiles of temperature ~~profile~~ and ~~to surface temperature (bottom symbol in~~ of the ~~plot). Panels~~ $H_2O$ VMR profiles are plotted in panels (b) and (~~e~~d)~~refer to the $H_2O$ VMR and to the surface spectral emissivity profiles~~, respectively.

for emissivity, is constantly equal to 0.99 in all the 900 test runs. For surface temperature we obtain performances analogous to those of the temperature profile at the lowest atmospheric layers. For this reason, for simplicity, surface temperature differences and errors are not shown starting from Fig. 3.

Figure 4 shows the average differences between CDF and SR profiles (solid red lines). Dashed lines represent the average error of CDF (black) and SR (magenta) as evaluated from the error CMs of Eq's (10) and (18). Shadowed areas represent the standard deviations of the CDF minus SR differences. ~~As usual, panel~~ Panel (a) refers to the temperature profile, while panels (b) and (c) refer to the $H_2O$ VMR and surface spectral emissivity profiles, respectively. In this case of perfect matching of the measurements, we see that, on average, the differences between CDF and SR solutions are far smaller than the error estimated by the CMs. The standard deviation of the differences (shadowed area) is also much smaller than the error, thus we come to the important conclusion that the differences between the CDF and the SR solutions are much smaller than their associated error also in the individual test runs (not only on average). The very small size of the differences between the CDF and SR solutions

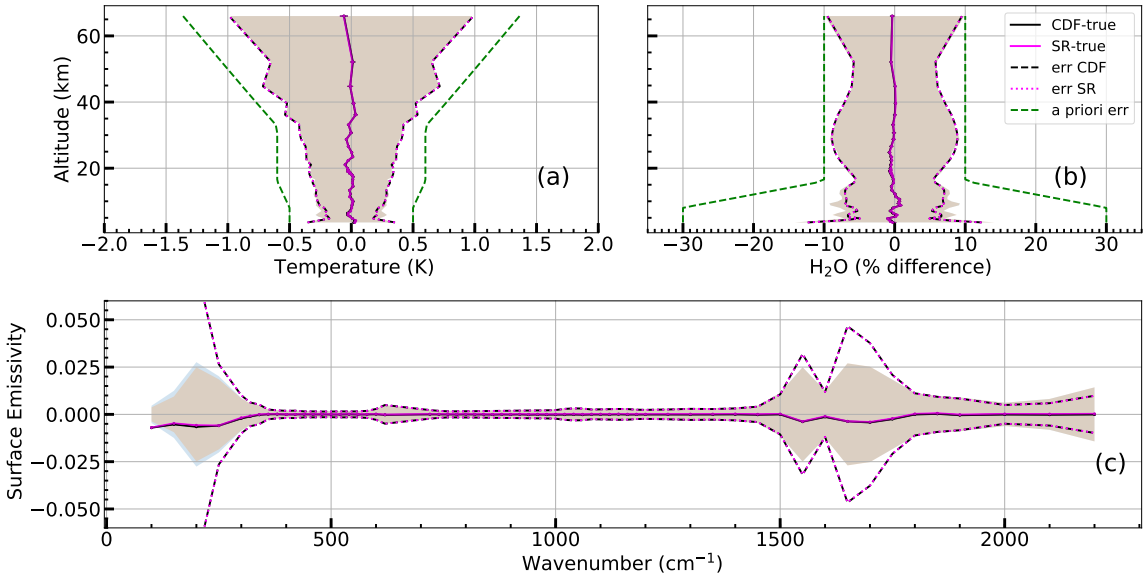


**Figure 3.** Case of perfectly matching measurements. Average differences between CDF and true profiles (black), and between SR and true (magenta) profiles. Dashed lines represent the average error of CDF (black) and of SR (magenta) as evaluated from the error CMs of Eq's (10) and (18). Shadowed areas represent the standard deviations of the differences, error bars are the standard errors of the average differences. Panel (a) refers to the temperature profile. Panels (b) and (c) refer to the $H_2O$ VMR and surface spectral emissivity profiles, respectively.

implies that the forward model linear approximation used in the the CDF is actually very accurate, at least for the FORUM and IASI-NG ~~Antarctic~~ measurements that we examined.

### 5.2 Results in case of measurement mismatch

In the second part of the study, we proceed with the same approach adopted for the first set of tests, however, we also introduce a space and time mismatch between the measurements of FORUM and IASI-NG. In this case, we reproduce an idealized scenario in which both instruments measure, for nine hundred times, a limited area of the Antarctic Plateau surface. The matching of the measurements is not perfect: according to the requirements mentioned earlier, FORUM and IASI-NG measurements are acquired within one minute from each other and sound, randomly, air masses and surface areas located within an horizontal distance of 26 km from each other. In each of the measurements the sounded atmosphere and the surface temperature change stochastically with respect to the reference $\mathbf{x}_0$, according to the local seasonal variability represented by the CM $\mathbf{S}_S$. The spectral emissivity of the surface spot sounded by FORUM is always that of the coarse snow model of Huang et al. (2016) while, to emulate the measurement mismatch, for IASI-NG the emissivity model is that of the medium snow model from the same authors. As usual, the synthetic noise applied to the measurements also changes from measurement to measurement. As

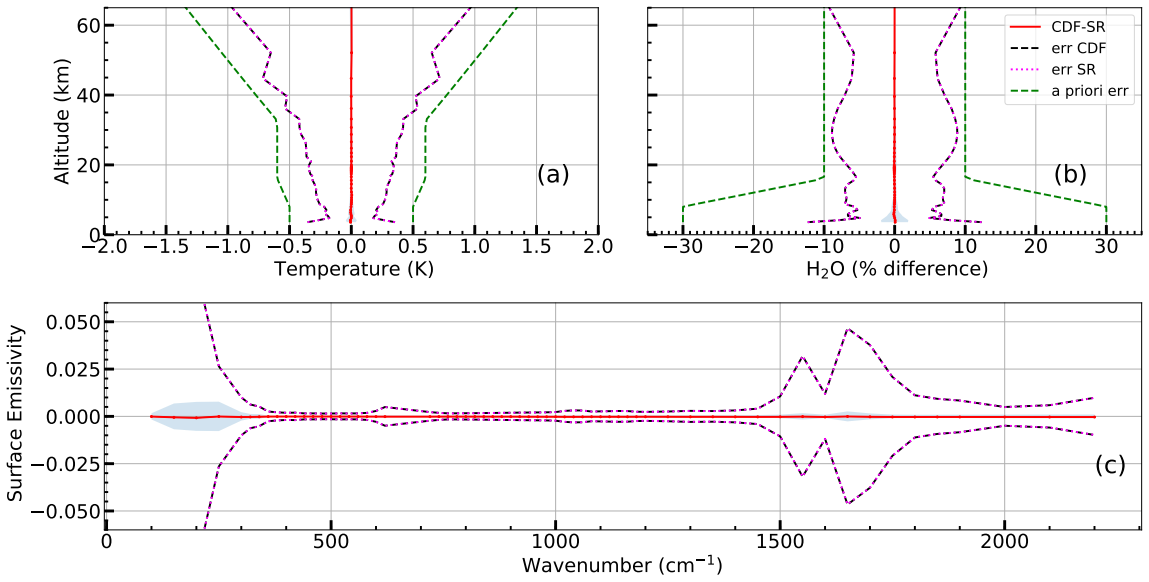


**Figure 4.** Case of perfectly matching measurements. Average differences between CDF and SR profiles (red). Dashed lines represent the average error of CDF (black) and of SR (magenta) as evaluated from the error CMs of Eq's (10) and (18). Shadowed areas represent the standard deviations of the CDF minus SR differences. Panel (a) refers to the temperature profile. Panels (b) and (c) refer to the $H_2O$ VMR and surface spectral emissivity profiles, respectively.

in the first set of tests, the a priori atmospheric and surface states are thought to be extracted from a source like the ECMWF analyses, thus they still change from a pair of FORUM and IASI-NG measurements to another, however, the same a priori data are used to process a given pair of measurements.

~~More in detail, we repeat~~ Note that, even if the atmospheres and the surface pixels sounded by the two measurements are different, we still assume as homogeneous the individual field of views (FOV) of the two instruments. This assumption is motivated by the fact that so far, at least for the FORUM sensor, the response to a non-uniformly illuminated FOV is not known. Moreover, the simulation of FOV inhomogeneities would require an atmospheric model with a spatial resolution in the order of ≈2 km, thus, the generation of a statistically significant set of synthetic observations would be extremely demanding from the computational point of view.

In detail, for $j = 1, \ldots, 900$ times, we repeat the following procedure. We generate ~~two~~ the surface temperature and the atmospheric state of the FORUM *true* state ~~vectors $\mathbf{x}_{t1}$ and $\mathbf{x}_{t2}$ using $\mathbf{T}(p)$, $T_s$, $\mathbf{x}_{H2O}(p)$ and $\mathbf{x}_{O3}(p)$ obtained by applying two different random perturbations~~ $\mathbf{x}_{t1,j}$ by applying a random perturbation to the reference $\mathbf{x}_0$. The applied ~~perturbations are~~ perturbation is taken from a multi-variate statistical distribution with zero average and ~~covariance equal to $\mathbf{S}_M/2$. Note that, since two independent perturbations are used to get $\mathbf{x}_{t1}$ and $\mathbf{x}_{t2}$, each of the perturbations must be consistentwith~~ CM

$\mathbf{S}_S$, representing the local seasonal variability. The *true* state $\mathbf{x}_{t2,j}$ sounded by IASI-NG and the ~~covariance $\mathbf{S}_M/2$ to get a difference $\mathbf{x}_{t1} - \mathbf{x}_{t2}$ with zero average and covariance equal to~~ a priori state $\mathbf{x}_a$ are then obtained by applying to $\mathbf{x}_{t1,j}$ two different perturbations consistent, respectively, with the mismatch CM $\mathbf{S}_M$ ~~. We assume the~~ and with the a priori CM $\mathbf{S}_{a,j}$. Regarding the *true* surface spectral emissivity~~of coarse snow for FORUM and of medium snow for IASI-NG. Assuming $\mathbf{x}_{t1}$ and $\mathbf{x}_{t2}$ we then generate FORUM and~~ , in all the test runs, for FORUM we assume the coarse snow model of Huang et al. 2016 and for IASI-NG ~~synthetic observations, respectively. As a priori estimates for surface temperature and for the profiles of temperature, $H_2O$ and $O_3$ VMRs, for this pair of measurements, we use values obtained by applying a random perturbation consistent with $\mathbf{S}_a$ to their reference value in $\mathbf{x}_0$~~the medium snow model. The a priori emissivity estimate is constant versus wavenumber and equal to 0.99. Assuming $\mathbf{x}_{t1,j}$ and $\mathbf{x}_{t2,j}$, we then generate FORUM and IASI-NG synthetic observations, respectively. Finally, we carry out the retrievals from FORUM-only, IASI-NG-only and FORUM+IASI-NG (~~synergistic, $\hat{\mathbf{x}}$~~$\hat{\mathbf{x}}_j$, synergistic) measurements and compute the CDF result ~~$\mathbf{x}_f$~~ $\mathbf{x}_{f,j}$ starting from FORUM-only and IASI-NG-only retrieved state vectors. In this case ~~, we carry out the SR using $\mathbf{S}'_{y2}$~~ the SR uses $\mathbf{S}'_{y2,j}$ given by Eq. (14) and, in the CDF, we attribute to ~~$\hat{\mathbf{x}}_2$ the error $\mathbf{S}'_{n,2}$~~ $\hat{\mathbf{x}}_{2,j}$ the error $\mathbf{S}'_{n,2,j}$ obtained from Eq. (20).

After these 900 runs, we compute the statistics of the differences between the synergistic / fused results and their true values used for the generation of synthetic observations.

Figure 5 is the analogous of Fig. 3 for the case of not perfectly matching measurements. We see that the bias of both CDF and SR solutions is still much smaller than the estimated error. As expected, ~~this~~ the latter (dashed lines) is slightly increased as compared to the case of perfectly matching measurements, this effect is especially visible for spectral emissivity. We note that, for wavenumbers above 1700 $\mathrm{cm}^{-1}$, the emissivity error of the CDF solution is slightly larger than that of the SR. This difference can be attributed to the different handling of the mismatch error in the CDF and SR approaches, as outlined in Sect. 2.3.

Figure 6 characterizes the differences between CDF and SR solutions in the presence of a mismatch between the measurements. This figure is to be compared to Fig. 4 that refers to perfectly coincident measurements. We see that, even in the presence of a mismatch, the average differences between the CDF and SR solutions are much smaller than their estimated error. Note, however, that in this case the standard deviation of the spectral emissivity differences between CDF and SR may ~~be as large as~~ approach the estimated error. This means that in each individual test run, the difference between the CDF and SR solutions may be ~~as large as~~ of the same order of the error estimated from the CMs (10) and (18). Again, since these differences do not exist in the case of perfectly matching measurements, they are to be attributed to the different treatment of the mismatch error in the CDF and SR approaches.

## 6 Conclusions

~~For a specific test scenario, we characterized~~ In this work, we characterize the differences between Synergistic Retrieval (SR) and Complete Data Fusion (CDF) techniques that may be used to generate synergistic products from independent remote-sensing measurements of the same airmass / ground pixel.

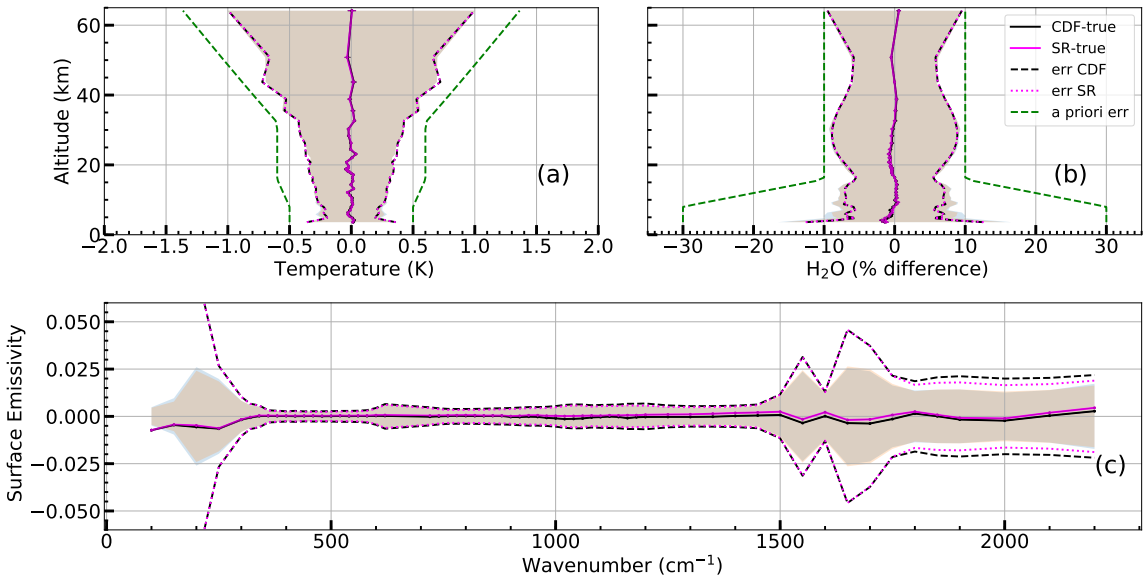


**Figure 5.** Case of not perfectly matching measurements. Average differences between CDF and true profiles (black), and between SR and true profiles (magenta). Dashed lines represent the average error of CDF (black) and SR (magenta) as evaluated from the error CMs of Eq's (10) and (18). Shadowed areas represent the standard deviations of the differences, error bars are the standard errors of the average differences. Panel (a) refers to the temperature profile. Panels (b) and (c) refer to the $H_2O$ VMR and surface spectral emissivity profiles, respectively.

Our assessment is based on synthetic upwelling spectral radiance measurements of the FORUM (Far-infrared Outgoing Radiation Understanding and Monitoring) and the IASI-NG (Infrared Atmospheric Sounding Interferometer - New Generation) missions that will be operational in a few years, from two different polar orbiting satellites. The analysis is limited to clear sky conditions that are expected to be the most favourable to exploit the complementarity of the measurements considered.

The presented results rely on a solid statistics of 900 simulated observations (and related test retrievals) with perfect matching and of 900 simulated observations with a realistic time- and space- mismatch. The simulated spectral radiances are based on a winter atmospheric scenario over the Antarctic Plateau. The extremely dry atmosphere makes the FIR region (100 - 620 cm$^{-1}$) relatively transparent, so that surface spectral emissivity can be retrieved from FORUM measurements with errors smaller than 0.01 in the range from 300 to 600 cm$^{-1}$. Less favourable conditions that may be encountered at mid- and tropical- latitudes were also investigated, confirming the conclusions of the intercomparison presented here. Therefore, for brevity, the figures relating to the test experiments at mid- and tropical- latitudes are provided only as supplemental material.

For perfectly matching measurements, we find that the differences between the SR and CDF solutions are as small as 1/10 of their error due to the propagation of measurement noise. In the presence of a realistic "worst case" mismatch between

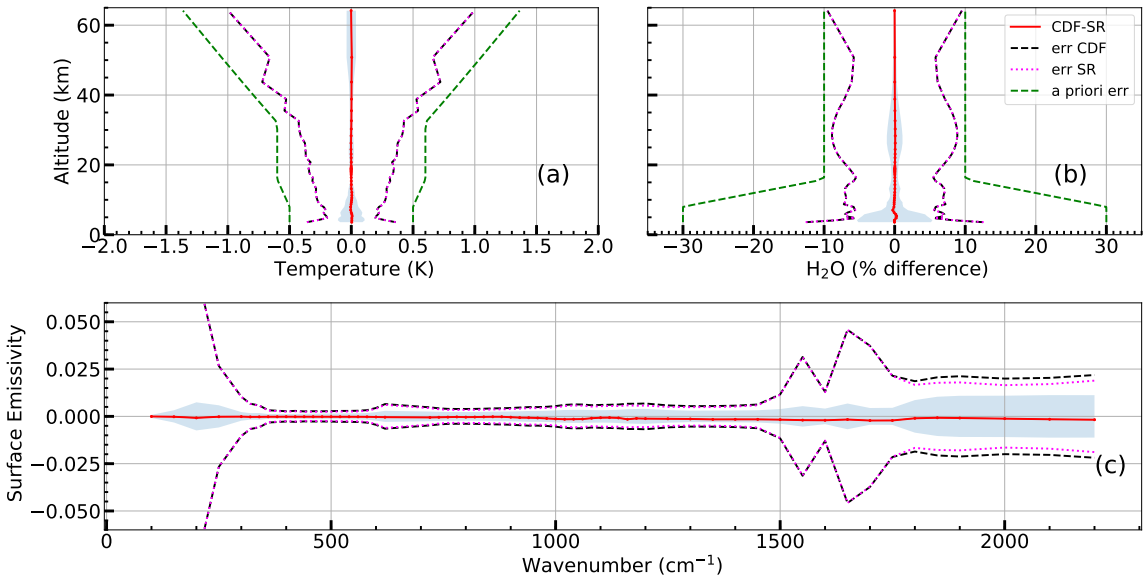


**Figure 6.** Case of not perfectly matching measurements. Average differences between CDF and SR profiles (solid red lines). Dashed lines represent the average error of CDF (black) and SR (magenta) as evaluated from the error CMs of Eq's (10) and (18). Shadowed areas represent the standard deviations of the CDF minus SR differences. Panel (a) refers to the temperature profile. Panels (b) and (c) refer to the $H_2O$ VMR and surface spectral emissivity profiles, respectively.

the soundings of the two instruments, the two techniques supply more different solutions. In this case, while the average differences are still much smaller than the error due to measurement noise, the SR and CDF solutions from individual pairs of measurements may show differences ~~as large as~~ approaching the errors due to noise. In our simulated experiment, the largest differences are observed in the spectral emissivity and for water vapour at the lowermost altitudes. Since these differences do not exist in case of perfectly matching measurements, they can not be ascribed to the forward model linear approximation made in the CDF. The difference is rather due to the different approaches of the two methods in handling the mismatch error.

As a conclusion, we confirm that SR and CDF provide equivalent results when applied to FORUM and IASI-NG complementary measurements. The final choice of which of the two approaches should be preferred for routine operations will depend on the actual architecture of the ground processors of the two missions. The SR approach requires the FORUM ground processor to access also the calibrated spectral radiances measured by IASI-NG with their error CMs, thus it implies a quite relevant throughput of data to be exchanged between the ground processors of the two missions. Conversely, the CDF technique is easily applied a posteriori using state vectors and diagnostic data derived from independent inversions of the individual measurements of the two missions. Despite its simplicity, a drawback of this latter technique originates from the fact that the two combined state vectors, being retrieved by two different mission processors (likely using different forward models), will

be affected by different model error components. Some of these components may be correlated, thus specific studies may be required to establish a reliable total error estimate of the fused state vector.

## 7 Author contributions

MR implemented the (synergistic) inversion code and carried-out the test retrievals presented. CT implemented the CDF algorithm in a computer program and computed the CDF solution for all the presented test cases. SC developed the theoretical background for the CDF. MR, CT and SC equally contributed to design the test scenarios, to the interpretation of the results, as well as to writing and revising the text of the paper. CB computed the atmospheric variability from ERA5 data and contributed to writing the paper. UC was the principal investigator of the AURORA H2020 project and the task coordinator of the OT4CLIMA project, both projects supported significantly the development of the CDF method. LP is the principal investigator of the FORUM mission and of the FORUM-science project that supported the presented studies. All the authors have revised and checked the text of the paper.

## 8 Data availability

~~Test data presented are available upon request to the authors~~The used reference atmospheres, the surface states and their variability, the mismatch error variance data and the noise error covariance matrices associated with the FORUM and IASI-NG measurements can be freely downloaded from Zenodo (Ridolfi et al., 2022). The dataset also includes all the relevant instrument characteristics and retrieval setup parameters assumed in the test experiments presented in this paper.

## Acknowledgements

The development of the CDF method was supported by the AURORA and OT4CLIMA projects. The AURORA project (http://www.aurora-copernicus.eu/) was supported by the Horizon 2020 research and innovation programme of the European Union (call: H2020-EO-2015; topic: EO-2-2015) under grant agreement no. 687428. The OT4CLIMA project was funded by the Italian Ministry of Education, University and Research (D.D. 2261 del 6.9.2018, PON R&I 2014- 2020 and FSC). The SR from FORUM and IASI-NG measurements was set up and optimized in the frame of the "FORUM-scienza" (FORUM science) project, agreement No. 2019-20-HH.0, funded by the Italian Space Agency in the 2019-2022 time frame.

## References


Agócs, T., Vanin, F., Laberinti, P., Oetjen, H., Serlenga, D., Sole, M. P., Salenc, C., Lamarre, D., Kaspers, M., Rodrigues, G., Carou, A. M., Strotmann, S., Copano, M., Lippa, M., and Morini, C.: Far-Infrared Outgoing Radiation Understanding and Monitoring (FORUM) – System Overview and Key Technology Developments of ESA's 9th Earth Explorer, in: IGARSS 2022 - 2022 IEEE International Geoscience and Remote Sensing Symposium, pp. 7186–7189, https://doi.org/10.1109/IGARSS46834.2022.9883892, 2022.

Aires, F., Aznay, O., Prigent, C., Paul, M., and Bernardo, F.: Synergistic multi-wavelength remote sensing versus a posteriori combination of retrieved products: Application for the retrieval of atmospheric profiles using MetOp-A, Journal of Geophysical Research: Atmospheres, 117, https://doi.org/10.1029/2011JD017188, _eprint: https://onlinelibrary.wiley.com/doi/pdf/10.1029/2011JD017188, 2012.

Amato, U., Masiello, G., Serio, C., and Viggiano, M.: The $\sigma$-IASI code for the calculation of infrared atmospheric radiance and its derivatives, Environmental Modelling & Software, 17, 651–667, https://doi.org/https://doi.org/10.1016/S1364-8152(02)00027-0, 2002.

Andrey-Andrés, J., Fourrié, N., Guidard, V., Armante, R., Brunel, P., Crevoisier, C., and Tournier, B.: A simulated observation database to assess the impact of the IASI-NG hyperspectral infrared sounder, Atmospheric Measurement Techniques, 11, 803–818, https://doi.org/10.5194/amt-11-803-2018, 2018.

Ben-Yami, M., Oetjen, H., Brindley, H., Cossich, W., Lajas, D., Maestri, T., Magurno, D., Raspollini, P., Sgheri, L., and Warwick, L.: Emissivity retrievals with FORUM's end-to-end simulator: challenges and recommendations, Atmospheric Measurement Techniques, 15, 1755–1777, https://doi.org/10.5194/amt-15-1755-2022, 2022.

Bermudo, F., Rousseau, S., Pequignot, E., and Bernard, F.: IASI-NG program: A new generation of Infrared Atmospheric Sounding Interferometer, in: 2014 IEEE Geoscience and Remote Sensing Symposium, pp. 1373–1376, https://doi.org/10.1109/IGARSS.2014.6946690, 2014.

Carnicero, D. B., Pachot, C., Oetjen, H., Mariani, F., Riel, S., Tromba, A., Lajas, D., Schuettemeyer, D., Sierk, B., Leveque, N., Kolm, M.-G., Korswagen, H., and Posselt, W.: The Far-Infrared Outgoing Radiation Understanding and Monitoring (Forum) Mission. ESA's 9th Earth Explorer, in: IGARSS 2020 - 2020 IEEE International Geoscience and Remote Sensing Symposium, pp. 6035–6038, https://doi.org/10.1109/IGARSS39084.2020.9323185, 2020.

Ceccherini, S., Carli, B., Cortesi, U., Del Bianco, S., and Raspollini, P.: Retrieval of the vertical column of an atmospheric constituent from data fusion of remote sensing measurements, Journal of Quantitative Spectroscopy and Radiative Transfer, 111, 507–514, https://doi.org/10.1016/j.jqsrt.2009.09.001, 2010a.

Ceccherini, S., Cortesi, U., Del Bianco, S., Raspollini, P., and Carli, B.: IASI-METOP and MIPAS-ENVISAT data fusion, Atmospheric Chemistry and Physics, 10, 4689–4698, https://doi.org/10.5194/acp-10-4689-2010, 2010b.

Ceccherini, S., Carli, B., and Raspollini, P.: Equivalence of data fusion and simultaneous retrieval, Optics Express, 23, 8476, https://doi.org/10.1364/OE.23.008476, 2015.

Ceccherini, S., Carli, B., Tirelli, C., Zoppetti, N., Del Bianco, S., Cortesi, U., Kujanpää, J., and Dragani, R.: Importance of interpolation and coincidence errors in data fusion, Atmospheric Measurement Techniques, 11, 1009–1017, https://doi.org/10.5194/amt-11-1009-2018, 2018.

Clerbaux, C. and Crevoisier, C.: New Directions: Infrared remote sensing of the troposphere from satellite: Less, but better, Atmospheric Environment, 72, 24–26, https://doi.org/https://doi.org/10.1016/j.atmosenv.2013.01.057, 2013.

Cortesi, U., Del Bianco, S., Ceccherini, S., Gai, M., Dinelli, B. M., Castelli, E., Oelhaf, H., Woiwode, W., Höpfner, M., and Gerber, D.: Synergy between middle infrared and millimeter-wave limb sounding of atmospheric temperature and minor constituents, Atmospheric Measurement Techniques, 9, 2267–2289, https://doi.org/10.5194/amt-9-2267-2016, 2016.

Costantino, L., Cuesta, J., Emili, E., Coman, A., Foret, G., Dufour, G., Eremenko, M., Chailleux, Y., Beekmann, M., and Flaud, J.-M.: Potential of multispectral synergism for observing ozone pollution by combining IASI-NG and UVNS measurements from the EPS-SG satellite, Atmospheric Measurement Techniques, 10, 1281–1298, https://doi.org/10.5194/amt-10-1281-2017, 2017.

Crevoisier, C., Clerbaux, C., Guidard, V., Phulpin, T., Armante, R., Barret, B., Camy-Peyret, C., Chaboureau, J.-P., Coheur, P.-F., Crépeau, L., Dufour, G., Labonnote, L., Lavanant, L., Hadji-Lazaro, J., Herbin, H., Jacquinet-Husson, N., Payan, S., Péquignot, E., Pierangelo, C., Sellitto, P., and Stubenrauch, C.: Towards IASI-New Generation (IASI-NG): impact of improved spectral resolution and radiometric noise on the retrieval of thermodynamic, chemistry and climate variables, Atmospheric Measurement Techniques, 7, 4367–4385, https://doi.org/10.5194/amt-7-4367-2014, 2014.

Cuesta, J., Eremenko, M., Liu, X., Dufour, G., Cai, Z., Höpfner, M., von Clarmann, T., Sellitto, P., Foret, G., Gaubert, B., Beekmann, M., Orphal, J., Chance, K., Spurr, R., and Flaud, J.-M.: Satellite observation of lowermost tropospheric ozone by multispectral synergism of IASI thermal infrared and GOME-2 ultraviolet measurements over Europe, Atmospheric Chemistry and Physics, 13, 9675–9693, https://doi.org/10.5194/acp-13-9675-2013, 2013.

Cuesta, J., Kanaya, Y., Takigawa, M., Dufour, G., Eremenko, M., Foret, G., Miyazaki, K., and Beekmann, M.: Transboundary ozone pollution across East Asia: daily evolution and photochemical production analysed by IASI + GOME2 multispectral satellite observations and models, Atmospheric Chemistry and Physics, 18, 9499–9525, https://doi.org/10.5194/acp-18-9499-2018, 2018.

Di Natale, G. and Palchetti, L.: Sensitivity studies toward the retrieval of ice crystal habit distributions inside cirrus clouds from upwelling far infrared spectral radiance observations, Journal of Quantitative Spectroscopy and Radiative Transfer, 282, 108 120, https://doi.org/https://doi.org/10.1016/j.jqsrt.2022.108120, 2022.

Di Natale, G., Palchetti, L., Bianchini, G., and Ridolfi, M.: The two-stream $\delta$-Eddington approximation to simulate the far infrared Earth spectrum for the simultaneous atmospheric and cloud retrieval, Journal of Quantitative Spectroscopy and Radiative Transfer, 246, 106 927, https://doi.org/https://doi.org/10.1016/j.jqsrt.2020.106927, 2020.

Fu, D., Worden, J. R., Liu, X., Kulawik, S. S., Bowman, K. W., and Natraj, V.: Characterization of ozone profiles derived from Aura TES and OMI radiances, Atmospheric Chemistry and Physics, 13, 3445–3462, https://doi.org/10.5194/acp-13-3445-2013, 2013.

Fu, D., Bowman, K. W., Worden, H. M., Natraj, V., Worden, J. R., Yu, S., Veefkind, P., Aben, I., Landgraf, J., Strow, L., and Han, Y.: High-resolution tropospheric carbon monoxide profiles retrieved from CrIS and TROPOMI, Atmospheric Measurement Techniques, 9, 2567–2579, https://doi.org/10.5194/amt-9-2567-2016, 2016.

Hersbach, H., Bell, B., Berrisford, P., Hirahara, S., Horányi, A., Muñoz-Sabater, J., Nicolas, J., Peubey, C., Radu, R., Schepers, D., Simmons, A., Soci, C., Abdalla, S., Abellan, X., Balsamo, G., Bechtold, P., Biavati, G., Bidlot, J., Bonavita, M., De Chiara, G., Dahlgren, P., Dee, D., Diamantakis, M., Dragani, R., Flemming, J., Forbes, R., Fuentes, M., Geer, A., Haimberger, L., Healy, S., Hogan, R. J., Hólm, E., Janisková, M., Keeley, S., Laloyaux, P., Lopez, P., Lupu, C., Radnoti, G., de Rosnay, P., Rozum, I., Vamborg, F., Villaume, S., and Thépaut, J.-N.: The ERA5 global reanalysis, Quarterly Journal of the Royal Meteorological Society, 146, 1999–2049, https://doi.org/https://doi.org/10.1002/qj.3803, 2020.

Huang, X., Chen, X., Zhou, D. K., and Liu, X.: An Observationally Based Global Band-by-Band Surface Emissivity Dataset for Climate and Weather Simulations, Journal of the Atmospheric Sciences, 73, 3541 – 3555, https://doi.org/10.1175/JAS-D-15-0355.1, 2016.

Kuai, L., Worden, J., Kulawik, S., Bowman, K., Lee, M., Biraud, S. C., Abshire, J. B., Wofsy, S. C., Natraj, V., Frankenberg, C., Wunch, D., Connor, B., Miller, C., Roehl, C., Shia, R.-L., and Yung, Y.: Profiling tropospheric $CO_2$ using Aura TES and TCCON instruments, Atmospheric Measurement Techniques, 6, 63–79, https://doi.org/10.5194/amt-6-63-2013, 2013.

Landgraf, J. and Hasekamp, O. P.: Retrieval of tropospheric ozone: The synergistic use of thermal infrared emission and ultraviolet reflectivity measurements from space, Journal of Geophysical Research: Atmospheres, 112, https://doi.org/10.1029/2006JD008097, 2007.

Levenberg, K.: A METHOD FOR THE SOLUTION OF CERTAIN NON-LINEAR PROBLEMS IN LEAST SQUARES, Quarterly of Applied Mathematics, 2, 164–168, https://www.jstor.org/stable/43633451, publisher: Brown University, 1944.

Liuzzi, G., Masiello, G., Serio, C., Meloni, D., Di Biagio, C., and Formenti, P.: Consistency of dimensional distributions and refractive indices of desert dust measured over Lampedusa with IASI radiances, Atmospheric Measurement Techniques, 10, 599–615, https://doi.org/10.5194/amt-10-599-2017, 2017.

Marquardt, D. W.: An Algorithm for Least-Squares Estimation of Nonlinear Parameters, Journal of the Society for Industrial and Applied Mathematics, 11, 431–441, https://www.jstor.org/stable/2098941, publisher: Society for Industrial and Applied Mathematics, 1963.

Masiello, G., Serio, C., Liuzzi, G., Venafra, S., Maestri, T., Martinazzo, M., Amato, U., and Grieco, G.: $\sigma$-IASI, https://doi.org/10.5281/zenodo.7019991, 2022.

Natraj, V., Liu, X., Kulawik, S., Chance, K., Chatfield, R., Edwards, D. P., Eldering, A., Francis, G., Kurosu, T., Pickering, K., Spurr, R., and Worden, H.: Multi-spectral sensitivity studies for the retrieval of tropospheric and lowermost tropospheric ozone from simulated clear-sky GEO-CAPE measurements, Atmospheric Environment, 45, 7151 – 7165, https://doi.org/https://doi.org/10.1016/j.atmosenv.2011.09.014, 2011.

Naylor, D. A. and Tahic, M. K.: Apodizing functions for Fourier transform spectroscopy, J. Opt. Soc. Am. A, 24, 3644–3648, https://doi.org/10.1364/JOSAA.24.003644, 2007.

Norton, R. H. and Beer, R.: New apodizing functions for Fourier spectrometry, J. Opt. Soc. Am., 66, 259–264, https://doi.org/10.1364/JOSA.66.000259, 1976.

Norton, R. H. and Beer, R.: Errata: New Apodizing Functions For Fourier Spectrometry, J. Opt. Soc. Am., 67, 419–419, https://doi.org/10.1364/JOSA.67.000419, 1977.

Oetjen, H.: Report for Mission Selection: FORUM, Tech. Rep. ESA-EOPSM-FORM-RP-3549, European Space Agency, ESA, 2200 AG, Noordwijk, The Netherlands, https://esamultimedia.esa.int/docs/EarthObservation/EE9-FORUM-RfMS-ESA-v1.0-FINAL.pdf, 2019.

Pachot, C., Carnicero, B., Oetjen, H., Sierk, B., Mariani, F., Riel, S., Rodrigues, G., Copano, M., Carou, A. M., Palchetti, L., Lippa, M., Giaccari, P., Mastrandrea, C., Perron, G., Keim, C., and Kolm, M.-G.: The infrared Fourier transform spectrometer and the infrared imager instrument concepts for the FORUM mission, ESA's 9th Earth Explorer, in: Proc. SPIE 11530, Sensors, Systems, and Next-Generation Satellites XXIV, 115300D, https://doi.org/10.1117/12.2570867, 2020.

Palchetti, L., Brindley, H., Bantges, R., Buehler, S. A., Camy-Peyret, C., Carli, B., Cortesi, U., Del Bianco, S., Di Natale, G., Dinelli, B. M., Feldman, D., Huang, X. L., C.-Labonnote, L., Libois, Q., Maestri, T., Mlynczak, M. G., Murray, J. E., Oetjen, H., Ridolfi, M., Riese, M., Russell, J., Saunders, R., and Serio, C.: FORUM: unique far-infrared satellite observations to better understand how Earth radiates energy to space, Bulletin of the American Meteorological Society, pp. 1–52, https://doi.org/10.1175/BAMS-D-19-0322.1, 2020.

Remedios, J. J., Leigh, R. J., Waterfall, A. M., Moore, D. P., Sembhi, H., Parkes, I., Greenhough, J., Chipperfield, M. P., and Hauglustaine, D.: MIPAS reference atmospheres and comparisons to V4.61/V4.62 MIPAS level 2 geophysical data sets, Atmospheric Chemistry and Physics Discussions, 7, 9973–10 017, https://doi.org/10.5194/acpd-7-9973-2007, 2007.

Ridolfi, M., Del Bianco, S., Di Roma, A., Castelli, E., Belotti, C., Dandini, P., Di Natale, G., Dinelli, B. M., C.-Labonnote, L., and Palchetti, L.: FORUM Earth Explorer 9: Characteristics of Level 2 Products and Synergies with IASI-NG, Remote Sensing, 12, https://doi.org/10.3390/rs12091496, 2020.

Ridolfi, M., Tirelli, C., Ceccherini, S., Belotti, C., Cortesi, U., and Palchetti, L.: Reference atmosphere, surface, instrument datased used for the generation of test experiments presented in doi.org/10.5194/amt-2022-82, https://doi.org/10.5281/zenodo.7221069, 2022.

Rodgers, C. D.: Inverse methods for atmospheric sounding: theory and practice, no. 2 in Series on atmospheric, oceanic and planetary physics, World Scientific, Singapore, 2000.

Sgheri, L., Belotti, C., Ben-Yami, M., Bianchini, G., Carnicero Dominguez, B., Cortesi, U., Cossich, W., Del Bianco, S., Di Natale, G., Guardabrazo, T., Lajas, D., Maestri, T., Magurno, D., Oetjen, H., Raspollini, P., and Sgattoni, C.: The FORUM end-to-end simulator project: architecture and results, Atmospheric Measurement Techniques, 15, 573–604, https://doi.org/10.5194/amt-15-573-2022, 2022.

Tirelli, C., Ceccherini, S., Zoppetti, N., Del Bianco, S., Gai, M., Barbara, F., Cortesi, U., Kujanpää, J., Huan, Y., and Dragani, R.: Data Fusion Analysis of Sentinel-4 and Sentinel-5 Simulated Ozone Data, Journal of Atmospheric and Oceanic Technology, 37, 573–587, https://doi.org/10.1175/JTECH-D-19-0063.1, 2020.

Tirelli, C., Ceccherini, S., Zoppetti, N., Bianco, S. D., and Cortesi, U.: Generalization of the complete data fusion to multi-target retrieval of atmospheric parameters and application to FORUM and IASI-NG simulated measurements, Journal of Quantitative Spectroscopy and Radiative Transfer, 276, 107 925, https://doi.org/https://doi.org/10.1016/j.jqsrt.2021.107925, 2021.

Warner, J. X., Yang, R., Wei, Z., Carminati, F., Tangborn, A., Sun, Z., Lahoz, W., Attié, J.-L., El Amraoui, L., and Duncan, B.: Global carbon monoxide products from combined AIRS, TES and MLS measurements on A-train satellites, Atmospheric Chemistry and Physics, 14, 103–114, https://doi.org/10.5194/acp-14-103-2014, 2014.

Worden, J., Liu, X., Bowman, K., Chance, K., Beer, R., Eldering, A., Gunson, M., and Worden, H.: Improved tropospheric ozone profile retrievals using OMI and TES radiances, Geophysical Research Letters, 34, https://doi.org/10.1029/2006GL027806, 2007.

Worden, J. R., Turner, A. J., Bloom, A., Kulawik, S. S., Liu, J., Lee, M., Weidner, R., Bowman, K., Frankenberg, C., Parker, R., and Payne, V. H.: Quantifying lower tropospheric methane concentrations using GOSAT near-IR and TES thermal IR measurements, Atmospheric Measurement Techniques, 8, 3433–3445, https://doi.org/10.5194/amt-8-3433-2015, 2015.

Zoppetti, N., Ceccherini, S., Carli, B., Del Bianco, S., Gai, M., Tirelli, C., Barbara, F., Dragani, R., Arola, A., Kujanpää, J., van Peet, J. C. A., van der A, R., and Cortesi, U.: Application of the Complete Data Fusion algorithm to the ozone profiles measured by geostationary and low-Earth-orbit satellites: a feasibility study, Atmospheric Measurement Techniques, 14, 2041–2053, https://doi.org/10.5194/amt-14-2041-2021, 2021.